

WILEY-VCH

**Supporting Information**

**Sewing Machine Stitching of Polyvinylidene Fluoride Fibers: Programmable Textile Patterns for Wearable Triboelectric Sensors**

*Young-Eun Shin<sup>a</sup>, Jeong-Eun Lee<sup>b</sup>, Yoojeong Park<sup>a</sup>, Sang-Ha Hwang<sup>b</sup>, Han Gi Chae<sup>b\*</sup>, Hyunhyub Ko<sup>a\*</sup>*

<sup>a</sup>School of Energy and Chemical Engineering, Ulsan National Institute of Science and Technology (UNIST), 50 UNIST-gil, Ulsan 44919, Republic of Korea

<sup>b</sup>School of Materials Science and Technology, Ulsan National Institute of Science and Technology (UNIST), 50 UNIST-gil, Ulsan 44919, Republic of Korea

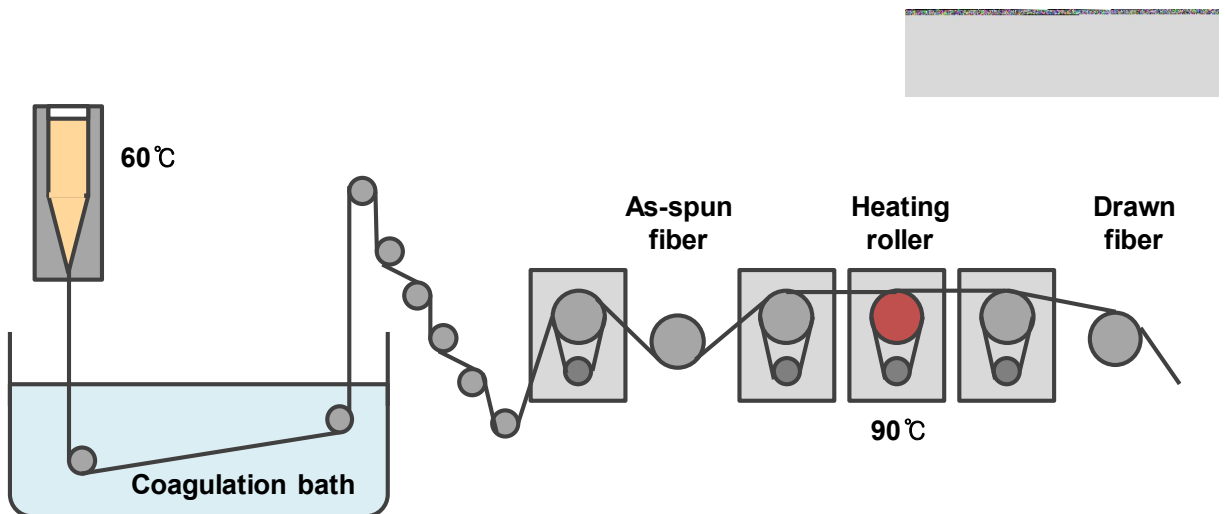


**Figure S1.** A schematic illustration of the lab scale dry-jet wet spinning procedure.

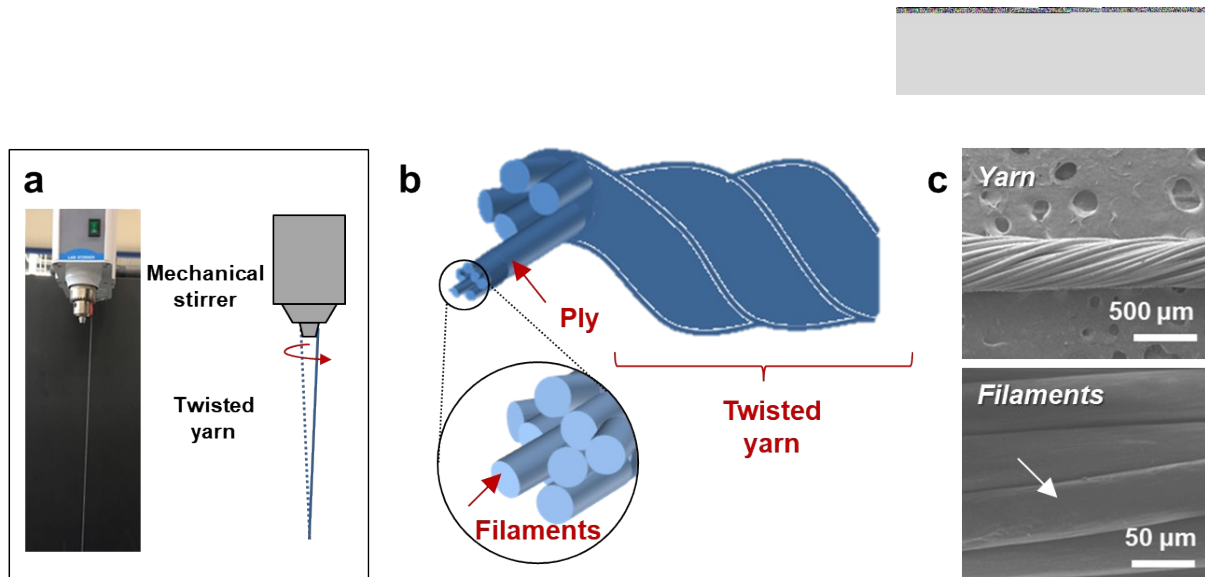


**Figure S2.** Twisting procedure for multi-ply PVDF yarn. (a) Photographic images of the twisting procedure. (b) A schematic illustration of the PVDF yarn composed of 40-filaments. (c) SEM images of PVDF yarn and filaments.

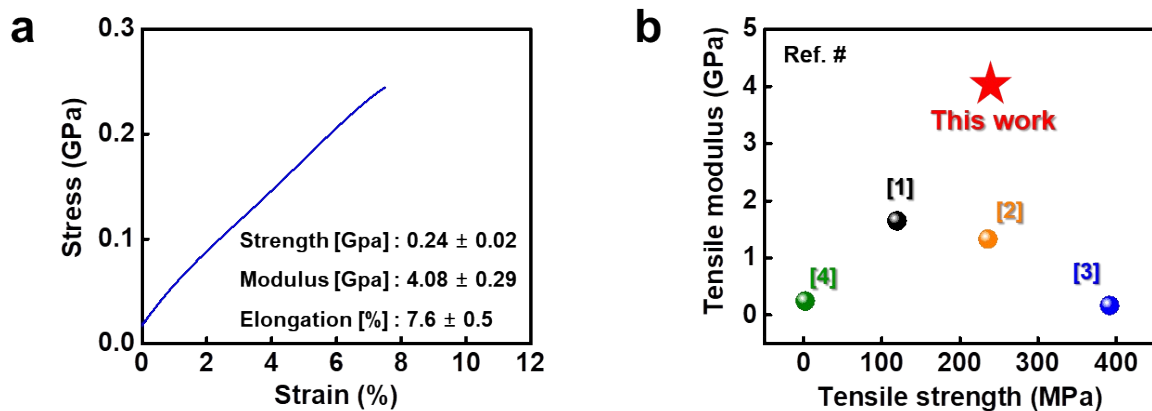


**Figure S3.** Mechanical characteristics of dry-jet wet-spun PVDF in this work; (a) Strain-stress curves, and (b) comparison of tensile modulus and strength based on this work and previous reports.

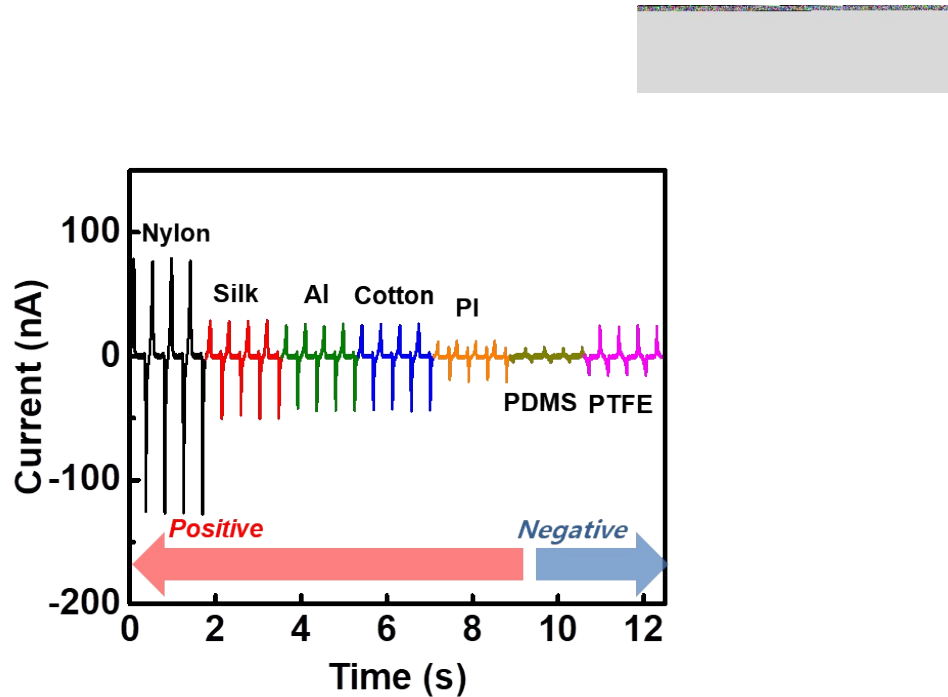


**Figure S4.** Triboelectric output current profiles of PVDF stitch textile sensor with relative contact-separation motion to different materials.

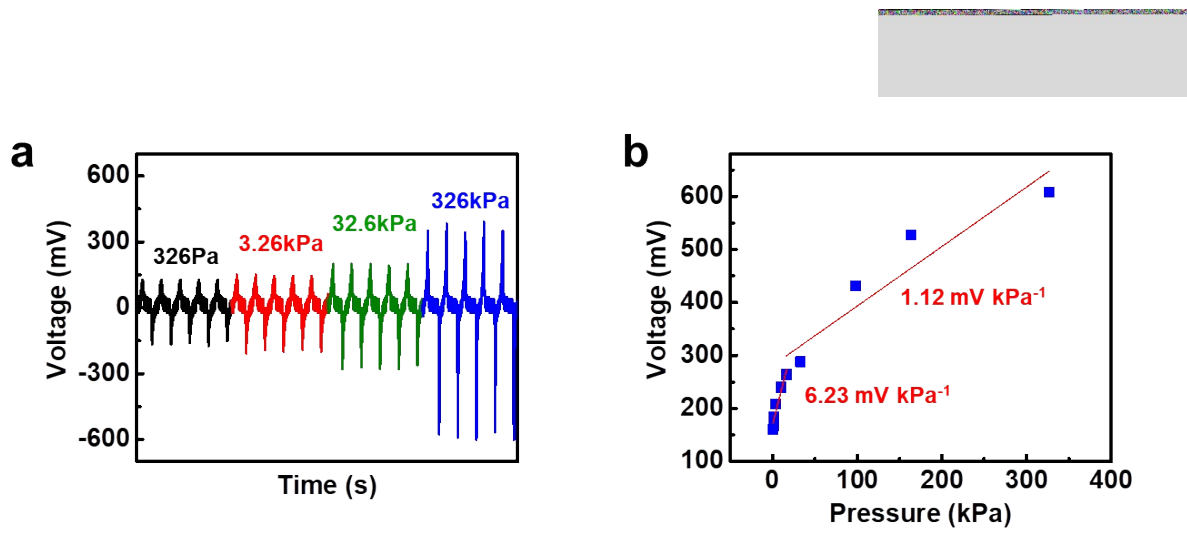


**Figure S5.** Evaluation of the PVDF stitch-based textile sensor for self-powered force sensing; (a) Triboelectric output voltage as a function of time at different pressures applied on the device. (b) Linear fitting between the triboelectric voltage variations and the applied pressure (326 Pa ~ 326 kPa).

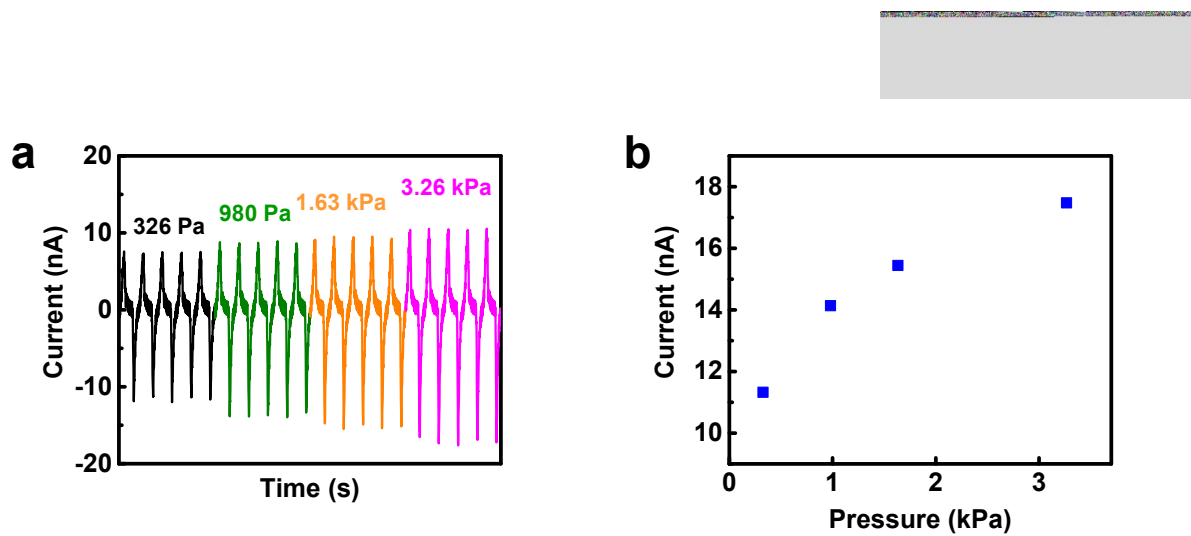


**Figure S6.** Triboelectric output signals in the low-pressure region (a) Triboelectric output current as a function of time and (b) the applied pressures from 326 Pa to 3.26 kPa in the low-pressure region.

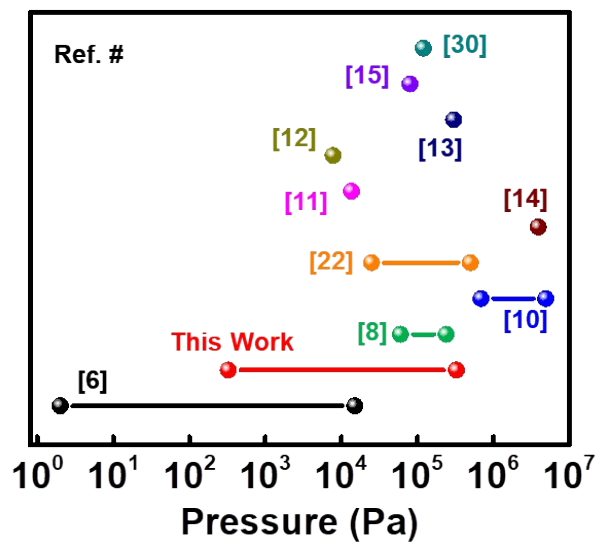


**Figure S7.** Comparison of the detectable pressure range of the results achieved in this work with previously reported triboelectric pressure sensor.



**Figure S8.** Washing durability of PVDF stitch textile sensor; Demonstration of the washing environment with commercial detergent by magnetic stirring.

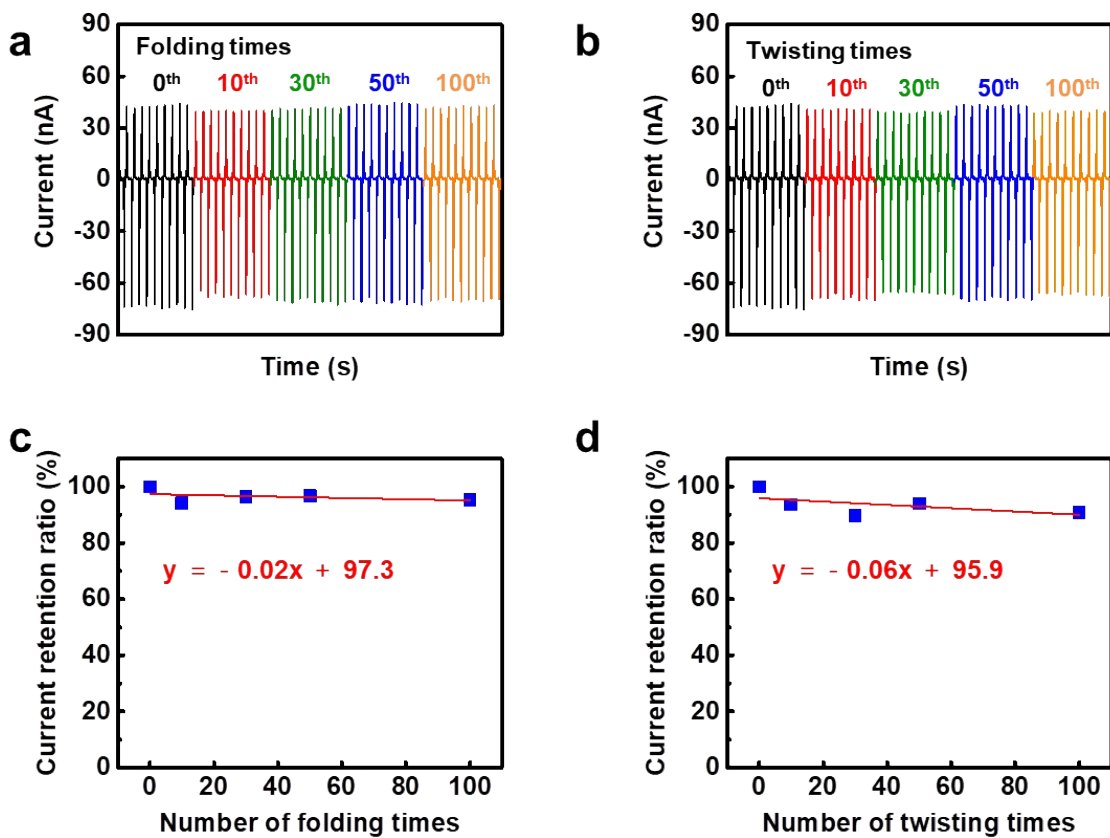


**Figure S9.** Evaluation of the PVDF stitch-based textile sensor for mechanical stability. (a, b)

Triboelectric output current of the device after 100 cycles of mechanical deformation by folding and twisting. (c, d) Change of the triboelectric current retention ratio as a function of the number of mechanical deformation.

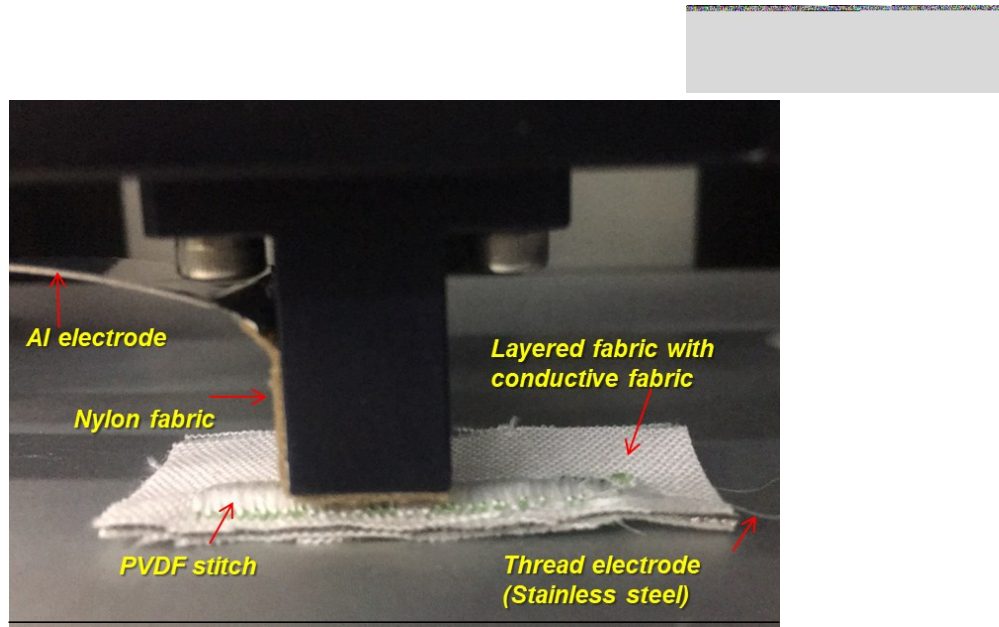


**Figure S10.** Experimental image of contact-separation motion between PVDF stitch and nylon fabric.

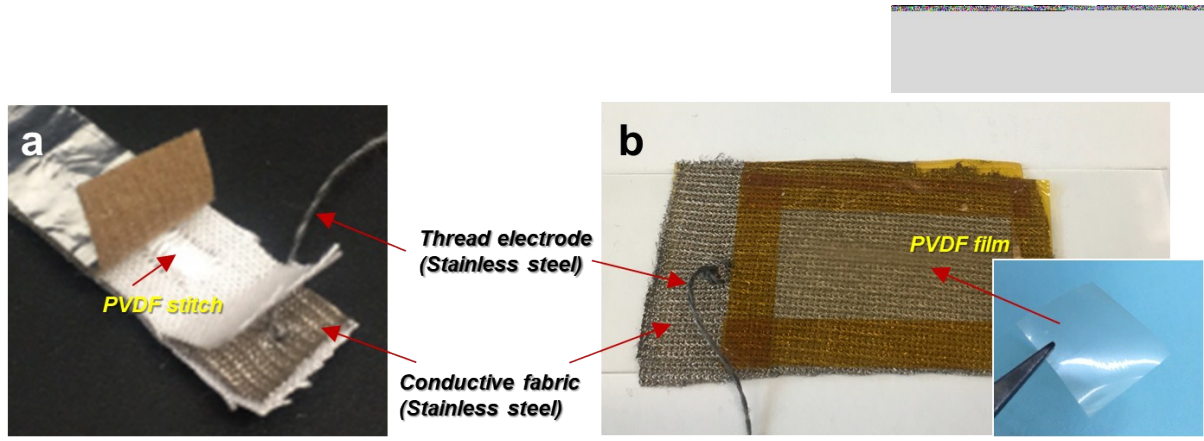


**Figure S11.** Comparison of both types of PVDF sensor. (a, b) Photographic images of (a) the stitch-based sensor and (b) the film-based sensor.

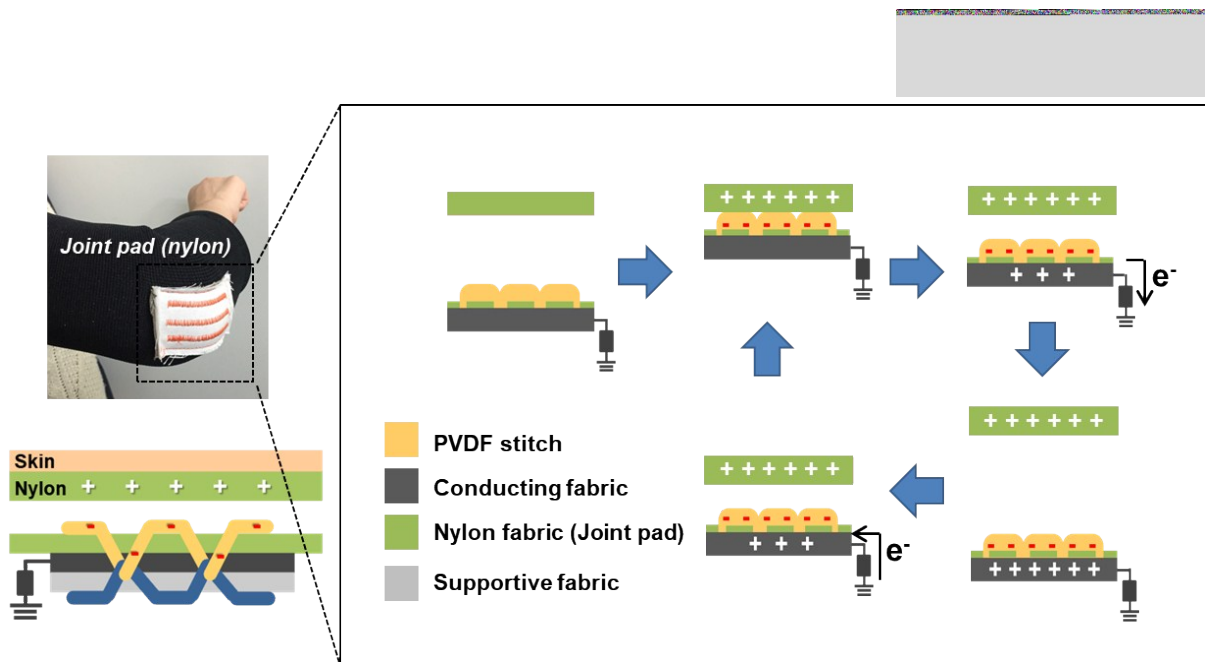


**Figure S12.** Working mechanism of PVDF stitch-based textile sensor as a body-motion sensor; Schematic illustration of triboelectric charge generation and electrons flow mechanism with single electrode system.

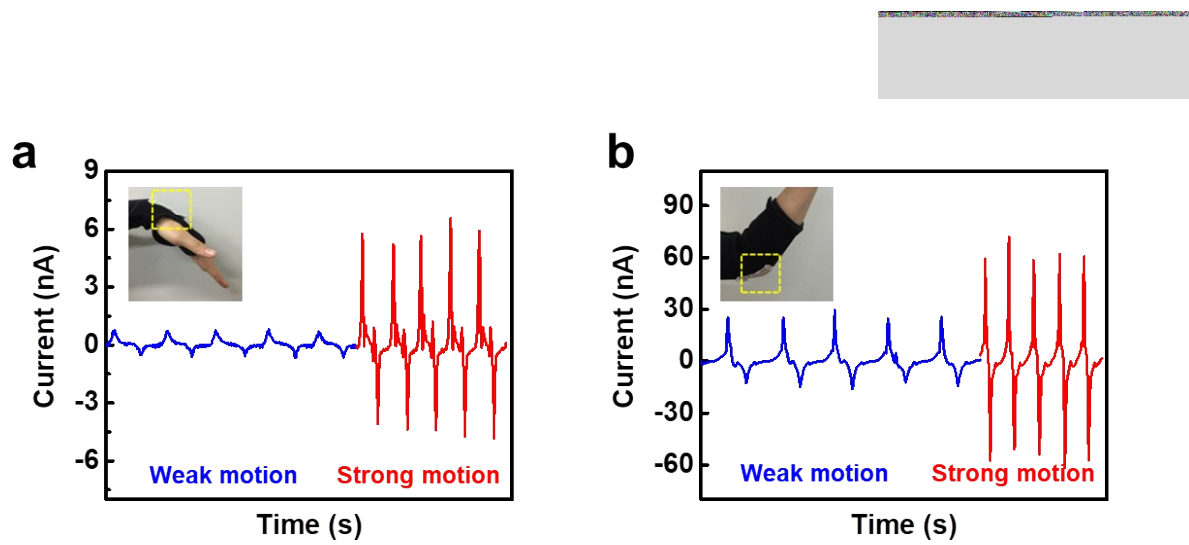


**Figure S13.** Real-time detection of body motion with different strength; (a) Output current signals from wrist movements with weak and strong motion. (b) Output current signals from elbow movements with weak and strong motion.

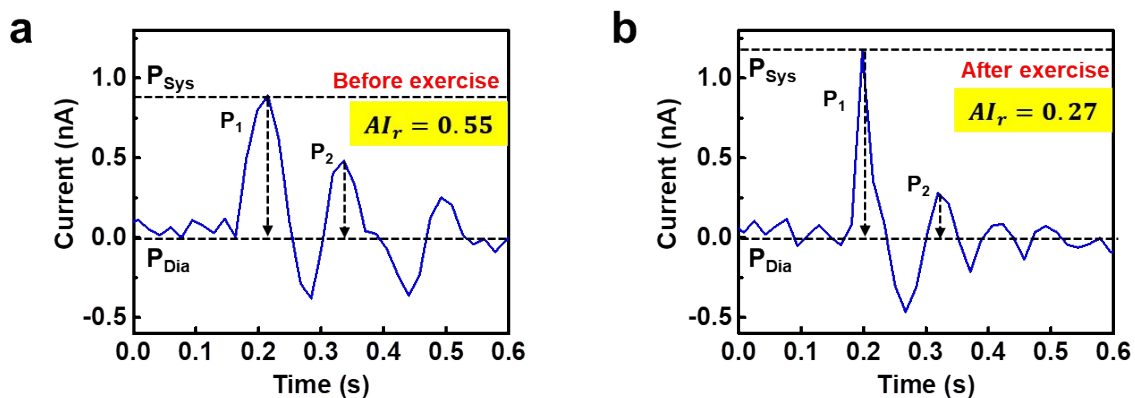
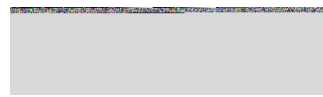


**Figure S14.** Comparison of augmentation index ( $AI_r$ ) before and after physical exercise.



**Table S1.** Comparison of mechanical characteristics of the results achieved in this work with previously reported as-spun PVDF fibers.

Fiber	Strength (GPa)	Young's modulus (GPa)
Melt-spun PVDF <sup>[1]</sup>	0.12	1.65
Melt-spun PVDF <sup>[2]</sup>	0.24	1.33
Electro-spun PVDF <sup>[3]</sup>	0.39	1.69
Electro-spun PVDF <sup>[4]</sup>	0.002	0.25
<b>Dry-jet wet-spun PVDF (this work)</b>	<b>0.24</b>	<b>4</b>



**Table S2.** Comparison of detection range of the results achieved in this work with previously reported textile-based sensors.

Textile fabrication	Basic materials	Detection range	Sensor type
Embedment	Cotton fabric coated CNT & Ni	2 Pa ~ 15 kPa	Resistive <sup>[5]</sup>
	Electrically Cu, Ni plating fabric, PE fabric	0.69 MPa ~ 4.9 MPa	Resistive <sup>[6]</sup>
	PET fabric with PDMS, CNT, Ag	40 kPa ~ 240 kPa	Triboelectric <sup>[7]</sup>
Hand weaving	Conductive thread stripes, synthetic elastic foam	~13.6 kPa	Capacitive <sup>[8]</sup>
	Conductive fabric, 3D textile	~ 7.8 kPa	Capacitive <sup>[9]</sup>
	Ag-coated textile, Proprietary Closed Cell Resin	~ 300 kPa	Capacitive <sup>[10]</sup>
Machine-weaving	Kevlar coaxial thread coated with SBS/AgNP	~ 3.9MPa	Capacitive <sup>[11]</sup>
	PVDF strap with electrode Hollow PDMS tube	~ 80kPa	Piezoelectric, Capacitive <sup>[12]</sup>
	Commercial stainless steel/PET fiber coated with PDMS	-	Triboelectric <sup>[13]</sup>
	PET fabric coated with Ni & Parylene	-	Triboelectric <sup>[14]</sup>
Machine-knitting	PET thread coated with Cu & PI	-	Triboelectric <sup>[15]</sup>
	Metallic stripes, semi conductive fabric	25 kPa ~ 500 kPa	Resistive <sup>[16]</sup>
Machine-knitting	Nylon fiber coated with graphene & nylon	-	Triboelectric <sup>[17]</sup>
Sewing machine stitching	Ag-coated conductive thread, 3D textile	~ 120 kPa	Capacitive <sup>[18]</sup>
	<b>As-spun PVDF on conductive fabric</b>	<b>326 Pa ~ 326 kPa</b>	<b>Triboelectric (This work)</b>



**Table S3.** Comparison of detection range and sensitivity of the results achieved in this work with previously reported triboelectric pressure sensors.

Type	Basic materials	Detection range	Sensitivity
Film <sup>[19]</sup>	PDMS, Al	0.6 ~ 30 MPa	$6 \text{ MPa}^{-1}$ (0.6 ~ 200kPa ), $0.037 \text{ MPa}^{-1}$ (350 kPa ~ 30 MPa)
Film <sup>[20]</sup>	PDMS, Liquid	0.4 ~ 40 N	$0.036 \text{ nA N}^{-1}$
Film <sup>[21]</sup>	PDMS, Al	1 ~ 150 kPa	$0.06 \text{ kPa}^{-1}$ (1~80 kPa)
Film <sup>[22]</sup>	PVDF-TrFE, PDMS	0.05 ~ 600 kPa	$104 \text{ mV kPa}^{-1}$ (0.05~5 kPa), $55 \text{ mV kPa}^{-1}$ (5~60 kPa), $49 \text{ mV kPa}^{-1}$ (60~600 kPa)
Film <sup>[23]</sup>	Cu/PDMS, PTFE	~50N	$0.019 \mu\text{A N}^{-1}$ (0 ~ 40 N)
Film <sup>[24]</sup>	PDMS	40 ~ 140 N	$28 \text{ mV N}^{-1}$
Textile <sup>[7]</sup> (embedding)	PET fabric with PDMS, CNT, Ag	40 kPa ~ 240 kPa	-
Textile (sewing machine stitching)	As-spun PVDF on conductive fabric	326 Pa ~ 326 kPa (9.8 mN ~ 9.8 N)	$0.66 \text{ nA kPa}^{-1}$ , $6.23 \text{ mV kPa}^{-1}$ (0.326 ~ 16.33 kPa), $0.1 \text{ nA kPa}^{-1}$ , $1.12 \text{ mV kPa}^{-1}$ (16.33 ~ 326 kPa)



**Table S4.** Comparison of fabrication conditions and washability of the results achieved in this work with previously reported textile-based sensors.

Fabrication	Key material	Electrode	Substrate	Delicate pattern	Washability	Sensor type
<b>Embedment in commercial thread or fabric</b>						
Coating	Carbonized silk	-	Silk fabric	-	-	Resistive <sup>[25]</sup>
CNT coating & Ni plating	CNT coated fabric & Ni	-	Cotton fabric	△	-	Resistive <sup>[5]</sup>
Stencil printing	Ag-fluoroelastomer	-	Knitted fabric (Nylon/PU)	△	○	Resistive <sup>[26]</sup>
Coating	PDMS, PET,	Aligned CNT, Ag paste	PET fabric	-	-	Triboelectric <sup>[7]</sup>
Coating	PDMS-AgNW, PTFE, PU-AgNW	AgNW	PU fiber	-	-	Triboelectric <sup>[27]</sup>
Layering	Cu, Ni- electroplating fabric, PE	Cu, Ni	PE fabric	-	-	Capacitive <sup>[6]</sup>
Layering	Conductive thread stripes, synthetic elastic foam	Conductive thread	Synthetic elastic foam	-	-	Capacitive <sup>[8]</sup>
Layering	Conductive fabric, 3D textile	Conductive fabric	Conductive fabric, 3D textile	-	-	Capacitive <sup>[9]</sup>
Layering	Ag-coated textile, Proprietary Closed Cell Resin	Ag	-	-	○	Capacitive <sup>[10]</sup>
<b>Conventional textile fabrication technique</b>						
Weaving (by hand)	PDMS	SBS/AgNP	Kevlar fiber	-	-	Capacitive <sup>[11]</sup>
	PVDF, PET	Metal	Elastic hollow tube	-	-	Piezoelectric, Capacitive <sup>[12]</sup>
	CNT & PTFE	CNT	Cotton thread	-	-	Triboelectric <sup>[28]</sup>
	PDMS, Au-coated Al	Au-coated ZnO NWs/Al wire	Al wire, Al foil	-	-	Triboelectric <sup>[29]</sup>
	PVDF-TrFE, Ag	CNT, Ag-coated nylon yarn	PU fiber	-	-	Triboelectric <sup>[30]</sup>
	PDMS, stainless-steel/PET thread	Stainless-steel/PET thread	Stainless-steel/PET thread	-	○	Triboelectric <sup>[13]</sup>
	Ni & parylene	Ni	PET fabric	-	-	Triboelectric <sup>[14]</sup>
Weaving (by Industrial weaving loom)	Cu, PI	Cu	PET thread	-	○	Triboelectric <sup>[15]</sup>
	Metallic stripes, semi-conductive fabric	Metallic stripes	Normal fabric	-	-	Resistive <sup>[16]</sup>

Fabrication	Key material	Electrode	Substrate	Delicate pattern	Washability	Sensor type
<b>Conventional textile fabrication technique</b>						
Knitting (by hand)	PDMS, stainless-steel/PET thread	Stainless steel/PET thread	Stainless steel/PET thread	-	○	Triboelectric <sup>[31]</sup>
Knitting (by Harry Lucas circular knitting machine)	CNT-wrapped spandex fiber	-	Spandex fiber	-	-	Resistive <sup>[32]</sup>
Knitting (by Industrial knitting machine)	PTFE thread, Ag thread	Ag thread	-	Plain-, double-, rib patterns	-	Triboelectric <sup>[33]</sup>
Knitting (by STOLL computerized flat knitting machine)	PTFE, Nylon	Graphene	Nylon fiber	-	-	Triboelectric <sup>[17]</sup>
Sewing (by hand)	Graphene nano platelets	-	Commercial yarn	-	-	Resistive <sup>[34]</sup>
Stitching (by sewing machine)	Ag/AgCl or carbon coated PET thread	Ag/AgCl or carbon coated PET thread	PET thread	△	-	Electro-chemical <sup>[35]</sup>
	Melt-spun coaxial polymer optical fiber	-	Polymer optical fiber	△	○	Photonic <sup>[36]</sup>
	Ag-coated conductive thread, 3D textile	Ag-coated conductive thread	Non-conductive textile	-	○	Capacitive <sup>[18]</sup>
	As-spun PVDF fiber	Ag conductive fabric	Various fabric (Cotton, Silk)	Various patterns, Letters, Embroidery	○	Triboelectric (This work)

**Movie S1.** Demonstration of the washing environment with commercial detergent by magnetic stirring.

**Movie S2.** Real-time detection of body motion (wrist).

**Movie S3.** Real-time detection of body motion (elbow).

**Movie S4.** Real-time detection of hand gestures.



## References

1. J. Yang, Q. Chen, F. Chen, Q. Zhang, K. Wang and Q. Fu, *Nanotechnology*, 2011, **22**, 355707.
2. A. Baji, Y.-W. Mai, M. Abtahi, S.-C. Wong, Y. Liu and Q. Li, *Compos. Sci. Technol.*, 2013, **88**, 1-8.
3. R. L. Hadimani, D. V. Bayramol, N. Sion, T. Shah, L. Qian, S. Shi and E. Siores, *Smart Mater. Struct.*, 2013, **22**, 075017.
4. J. Zheng, X. Yan, M.-M. Li, G.-F. Yu, H.-D. Zhang, W. Pisula, X.-X. He, J.-L. Duvail and Y.-Z. Long, *Nanoscale Res. Lett.*, 2015, **10**, 475.
5. M. Liu, X. Pu, C. Jiang, T. Liu, X. Huang, L. Chen, C. Du, J. Sun, W. Hu and Z. L. Wang, *Adv. Mater.*, 2017, **29**.
6. M. Inaba, Y. Hoshino, K. Nagasaka, T. Ninomiya, S. Kagami and H. Inoue, in Intelligent Robots and Systems' 96, IROS 96, Proceedings of the 1996 IEEE/RSJ International Conference on, Vol. 2, IEEE, 1996, 450-457.
7. L. Liu, J. Pan, P. Chen, J. Zhang, X. Yu, X. Ding, B. Wang, X. Sun and H. Peng, *J. Mater. Chem. A.*, 2016, **4**, 6077-6083.
8. M. Sergio, N. Manaresi, F. Campi, R. Canegallo, M. Tartagni and R. Guerrieri, *IEEE J. Solid-State Circuit*, 2003, **38**, 966-975.
9. T. Hoffmann, B. Eilebrecht and S. Leonhardt, *IEEE Sens. J.*, 2011, **11**, 1112-1119.
10. T. Holleczek, A. Rüegg, H. Harms and G. Tröster, *Sensors*, 2010 IEEE, IEEE: 2010, 2010, **732-737**.
11. J. Lee, H. Kwon, J. Seo, S. Shin, J. H. Koo, C. Pang, S. Son, J. H. Kim, Y. H. Jang and D. E. Kim, *Adv.Mater.*, 2015, **27**, 2433.
12. Y. Ahn, S. Song and K.-S. Yun, *Smart Mater. Struct.*, 2015, **24**, 075002.
13. K. Dong, J. Deng, Y. Zi, Y. C. Wang, C. Xu, H. Zou, W. Ding, Y. Dai, B. Gu and B. Sun, *Adv. Mater.*, 2017, **29**.
14. X. Pu, L. Li, M. Liu, C. Jiang, C. Du, Z. Zhao, W. Hu and Z. L. Wang, *Adv. Mater.*, 2016, **28**, 98.
15. Z. Zhao, C. Yan, Z. Liu, X. Fu, L. M. Peng, Y. Hu and Z. Zheng, *Adv. Mater.*, 2016, **28**, 10267.
16. J. Cheng, M. Sundholm, B. Zhou, M. Hirsch and P. Lukowicz, *Pervasive and Mobile Computing*, 2016, **30**, 97.
17. M. Zhu, Y. Huang, W. S. Ng, J. Liu, Z. Wang, Z. Wang, H. Hu and C. Zhi, *Nano energy*, 2016, **27**, 439.



18. J. Meyer, B. Arnrich, J. Schumm and G. Troster, *IEEE Sens. J.*, 2010, **10**, 1391.
19. X. Wang, M. Que, M. Chen, X. Han, X. Li, C. Pan and Z. L. Wang, *Adv. Mater.*, 2017, **29**.
20. Q. Shi, H. Wang, T. Wang and C. Lee, *Nano Energy*, 2016, **30**, 450.
21. X. Wang, H. Zhang, L. Dong, X. Han, W. Du, J. Zhai, C. Pan and Z. L. Wang, *Adv. Mater.*, 2016, **28**, 2896.
22. K. Parida, V. Bhavanasi, V. Kumar, R. Bendi and P. S. Lee, *Nano Res.*, 2017, **10**, 3557.
23. K. Y. Lee, H. J. Yoon, T. Jiang, X. Wen, W. Seung, S. W. Kim and Z. L. Wang, *Adv. Ener. Mater.*, 2016, **6**.
24. T. Li, J. Zou, F. Xing, M. Zhang, X. Cao, N. Wang and Z. L. Wang, *ACS nano* **2017**, **11**, 3950.
25. C. Wang, X. Li, E. Gao, M. Jian, K. Xia, Q. Wang, Z. Xu, T. Ren and Y. Zhang, *Adv. Mater.*, 2016, **28**, 6640.
26. H. Jin, N. Matsuhisa, S. Lee, M. Abbas, T. Yokota and T. Someya, *Adv. Mater.*, 2017, **29**.
27. Y. Cheng, X. Lu, K. H. Chan, R. Wang, Z. Cao, J. Sun and G. W. Ho, *Nano Energy* 2017, **41**, 511.
28. J. Zhong, Y. Zhang, Q. Zhong, Q. Hu, B. Hu, Z. L. Wang and J. Zhou, *ACS nano* 2014, **8**, 6273.
29. K. N. Kim, J. Chun, J. W. Kim, K. Y. Lee, J.-U. Park, S.-W. Kim, Z. L. Wang and J. M. Baik, *ACS nano* 2015, **9**, 6394.
30. H. J. Sim, C. Choi, S. H. Kim, K. M. Kim, C. J. Lee, Y. T. Kim, X. Lepró, R. H. Baughman and S. J. Kim, *Sci. Rep.*, 2016, **6**.
31. K. Dong, Y.-C. Wang, J. Deng, Y. Dai, S. L. Zhang, H. Zou, B. Gu, B. Sun and Z. L. Wang, *ACS nano* 2017, **11**, 9490.
32. J. Foroughi, G. M. Spinks, S. Aziz, A. Mirabedini, A. Jeiranikhahmeneh, G. G. Wallace, M. E. Kozlov and R. H. Baughman, *ACS nano* 2016, **10**, 9129.
33. S. S. Kwak, H. Kim, W. Seung, J. Kim, R. Hinchet and S.-W. Kim, *ACS nano* 2017.
34. J. J. Park, W. J. Hyun, S. C. Mun, Y. T. Park and O. O. Park, *ACS Appl. Mater. Interfaces*, 2015, **7**, 6317-6324.
35. X. Liu and P. B. Lillehoj, *Lab Chip* 2016, **16**, 2093-2098.
36. B. M. Quandt, F. Braun, D. Ferrario, R. M. Rossi, A. Scheel-Sailer, M. Wolf, G.-L. Bona, R. Hufenus, L. J. Scherer and L. F. Boesel, *J. R. Soc. Interface*, 2017, **14**, 20170060.